ELSEVIER

Journal of Alloys and Compounds 421 (2006) 156–162

Journal of ALLOYS AND COMPOUNDS

www.elsevier.com/locate/jallcom

Ignition and reaction mechanism of Co–Al and Nb–Al intermetallic compounds prepared by combustion synthesis

C. Milanese [a], F. Maglia [a,*], A. Tacca [a], U. Anselmi-Tamburini [a,b], C. Zanotti [c], P. Giuliani [c]

[a] *Department of Physical Chemistry, University of Pavia, V.le Taramelli 16, 27100 Pavia, Italy*
[b] *IENI-CNR, Department of Pavia, V.le Taramelli 16, 27100 Pavia, Italy*
[c] *IENI-CNR, Department of Milano, Via Cozzi 53, 20125 Milano, Italy*

Received 25 March 2005; accepted 29 August 2005
Available online 15 December 2005

Abstract

The ignition and propagation mechanism of the self-propagating high-temperature synthesis of several cobalt and niobium aluminides was investigated. Two propagation mechanisms were identified depending on the stoichiometry of the starting mixture. Al-rich compositions propagate through a dissolution–precipitation mechanism while Al-poor mixtures require solid state diffusion. The ignition temperatures were measured by means of microthermocouples in quasi-adiabatic conditions through experiments carried out in thermal explosion mode. Ignition temperatures were found to be characteristic of each system and to depend strongly on reactants particle size. Ignition energies for all compositions were evaluated through a mathematical model.

Keywords: Combustion synthesis; Intermetallics; Aluminides; Diffusion

1. Introduction

Intermetallic compounds and composite materials based on them are considered as prospective materials for various high-temperature and structural applications. In many cases they offer a unique combination of high-temperature mechanical properties and low density, even superior to nickel-based superalloys.

Transition metals aluminides exhibit fairly high melting points, good resistance to corrosion and oxidation at high temperatures, high mechanical strength, together with good chemical and thermal expansion compatibility with Al_2O_3 reinforcing fibers, that enable the fabrication of light weight and high creep strength composites [1–3]. Ni–Al is the most investigated system. Fewer studies have been devoted to the synthesis and characterization of other promising aluminides, such as the intermetallics in the Nb–Al [4–8] and Co–Al [9–13] systems.

Niobium aluminides are among the most refractory ones [14]: $NbAl_3$ melts at 1680 °C, while Nb_3Al and Nb_2Al decompose according to a peritectic reaction at 2060 and 1940 °C, respectively. $NbAl_3$ has a potential application as turbine blade material in aircraft engines and stationary gas turbine [15], thanks to its relatively low density (4.54 g/cm^3) and very good resistance to oxidation processes. Nb_3Al shows superconducting properties and has broad potential for alloying with transition metals as V, providing an opportunity for significant improvements of mechanical properties of Nb_3Al-based alloys [16].

Among the four Co–Al intermetallic compounds [17] only CoAl melts congruently (mp 1645 °C), while Co_2Al_9, Co_4Al_{13}, and Co_2Al_5 decompose according to peritectic reactions at temperatures ranging between 943 and 1170 °C. Cobalt aluminides are under investigation for their potential applications as metallization layers in III–V semiconductors devices [13]. Moreover, information about the solid–solid and solid–liquid reactivity between Co and Al and about the kinetics of formation of the Co–Al intermetallics would be particularly helpful in understanding the performance of tunnel junctions based on Co/Al_2O_3 interfaces used in electronic devices and of Co–Al multilayers used in magnetic recording heads and magnetic random access memories [10].

* Corresponding author. Tel.: +39 0382 987208; fax: +39 0382 987575.
E-mail address: filippo.maglia@unipv.it (F. Maglia).

0925-8388/$ – see front matter © 2005 Elsevier B.V. All rights reserved.
doi:10.1016/j.jallcom.2005.08.091

In general, conventional processing techniques used to synthesize high-temperature alloys, such as melting and casting methods, powder metallurgy, or more complex combinations of casting, powder grinding and consolidation by hot-pressing, have often faced problems for the fabrication of the intermetallic compounds due to the large differences in the melting points and in the densities between Al and the transition metals [18].

Some alternative processing techniques have been proposed, including mechanical alloying [19,20], single crystal growth [21] and combustion synthesis (also known as self-propagating high-temperature synthesis or SHS). Since the early 1970s, several transition metal aluminides [22], such as the ones in the Ni–Al [23,24] and Ti–Al [25,26] systems, have been obtained with this fast and low cost technique, thanks to the exothermicity of their formation reactions. To the authors' knowledge, only few papers deal with an investigation of the SHS processes in the Nb–Al system [27–29], while no works are devoted to the Co–Al ones.

The adiabatic combustion temperature (T_{ad}) is known only for the formation reaction of the phases $NbAl_3$ and CoAl. In both cases it is equal to the melting points T_m of the corresponding aluminide [24,30]. According to Maslov et al. [29], preheating of the starting mixture, prior to ignition, was necessary in order to react all the Nb–Al compositions. Only the phase $NbAl_3$ could be obtained in pure form starting from the corresponding Nb:Al = 1:3 mixture, while the other two compositions (Nb:Al = 1:2 and Nb:Al = 3:1) produced a mixture of Nb_2Al, $NbAl_3$ and unreacted Nb. The Nb_3Al phase was never observed in the products [27,29].

The aim of this work is to further our understanding of the fundamental aspects of the self-propagating synthesis of the intermetallics in the binary systems Co–Al and Nb–Al with particular focus on the ignition of the combustion reaction.

2. Experimental procedure

Elemental powders of the reactants (Table 1) were dry mixed in stoichiometric ratios corresponding to the following intermetallic phases: CoAl, Co_2Al_5, Co_2Al_9, Nb_3Al, Nb_2Al, and $NbAl_3$. The powder mixtures were then cold-pressed to form cylindrical pellets with a diameter of 10 mm and a height of 10–15 mm. The experiments were carried out in a stainless steel vacuum reactor under a high purity argon atmosphere (99.998%). Ignition of the reaction was accomplished by heat radiated from an electrically heated tungsten coil placed 1 mm away from one end of the sample. More details on the experimental apparatus are reported elsewhere [31].

When necessary, samples were preheated at 400 °C before ignition by using a Ni–Cr cylindrical wound-wire furnace, 25 mm in diameter and 30 mm high, placed around the pellets.

Table 1
Starting materials characteristics

Element	Supplier	Catalog no.	Grain size	Stated purity (%)
Co	Aldrich	26,663-9	<2 μm	99.8
Co	Aldrich	26,664-7	−100mesh (<149 μm)	>99.9
Nb	Aldrich	26,272-2	−325mesh (<44 μm)	99.8
Nb	Aldrich	26,274-9	−60mesh (<250 μm)	99.8
Al	Aldrich	21,475-2	−200mesh (<74 μm)	99

Temperature profiles were measured with a two-color pyrometer, with a resolution time of 0.01 s, focused on the middle of the sample, while the combustion wave velocities were determined from video recordings of the front displacement using a time code generator.

The analysis of the ignition process was carried out to determine the experimental parameters assuring the possibility to reach the ignition condition. The temperature history of the heated pellets was determined using small powder compacts, 6 mm in diameter and less than 1 mm high, with density values ranging from 2.5 to 4.5 g/cm^3 for the Co–Al system and from 3.5 to 5.5 g/cm^3 for the Nb–Al one. The size and the density of the pellets were chosen in order to obtain temperature homogeneity in the whole sample during the heating transient.

Pellets were heated by a CO_2 laser system, set to different powers, and the laser beam was focused on the upper face of the pellet in order to deposit the radiant energy on the whole surface.

Temperature profiles were acquired with a type S thermocouple (bead size of 50 μm, 10 ms response time) placed in the middle of the pellet and pressed with the reactant powders. The pellet was suspended (no holder in touch with the sample) in a reaction chamber by the thermocouple wires to reduce the heat loss by conduction. More details are given in [32].

Structural and microstructural characterization of reactants and products were made by scanning electron microscopy (SEM), energy dispersion electron microprobe (EDS), and powder X-ray diffraction (XRPD). A Zeiss Axioplan optical microscope and a Cambridge SEM Stereoscan 200 operated at 30 kV and equipped with a back-scattered electron detector and a Link microprobe were used. XRPD analysis was performed using a diffractometer Philips 1710 equipped with a copper anode (operated at 40 kV and 35 mA), graphite curved monochromator on the diffracted beam, and a proportional counter.

3. Results and discussion

3.1. Combustion synthesis

The combustion mode for the reactions of the Nb–Al system depends strongly on the Nb/Al ratio. The composition Nb:Al = 1:3 reacted in a stationary mode for both the Nb grain sizes (Table 1) with a combustion front temperature approximately equal to the $NbAl_3$ melting point (1680 °C). On the contrary, the compositions richer in Nb (Nb:Al = 2:1 and Nb:Al = 3:1) required pre-heating in order to ignite and propagate. The measured peak temperatures were, respectively, 1510 and 1480 °C, when a pre-heating temperature of 400 °C was used.

Melting of Al was visually observable for all compositions as it caused the expulsion from the pellet surface of some liquid spherical drops. Melting of Al shortly precedes the passage of the reactive front that causes the re-absorption of the Al droplets from the pellet surface. By XRPD analysis it was possible to verify that no conversion of reactants into products takes place after Al melting before the passage of the combustion front.

XRPD analyses performed on the fully reacted samples indicated that Nb:Al = 1:3 blends produced a single phase ($NbAl_3$) product, independently of Nb grain size. On the contrary, Nb:Al = 2:1 and Nb:Al = 3:1 compositions produced polyphasic products where Nb_2Al is the most conspicuous phase but also $NbAl_3$ and traces of Nb_3Al are present, together with unreacted Al and Nb (Table 2). Smaller amounts of secondary phases were obtained using finer Nb powders.

To investigate the chemical mechanism responsible for the combustion process some reactions were quenched when the combustion front had propagated halfway through the sample.

Table 2
Phase composition of the products obtained using starting compositions corresponding to all compounds present in the Nb–Al phase diagram

Phases in product	Starting mixture stoichiometry Nb:Al		
	1:3	2:1	3:1
Al	–	m	m
$NbAl_3$	M	m	m
Nb_2Al	–	M	M
Nb_3Al	–	t	t
Nb	–	M	M

Relative abundance: M, major; m, minor; t, trace.

This was accomplished by dropping the partially reacted pellet in water. Although the reaction cannot be instantaneously frozen, such experiments provide useful information on the phase evolution during the passage of the reaction front and on the microscopic mechanism of the SHS process. The quenched samples were prepared using the coarser Nb powders to facilitate SEM/EMPA analyses of the product phases.

Fig. 1a shows a back scattered electrons (BSE) low magnification image of the zone across the quenched front for the Nb:Al = 1:3 composition. The arrow indicates the direction of propagation of the combustion front quenched at the position indicated by the dashed line. In the region ahead of the reaction front (Fig. 1b) the dark Al grains and the light Nb grains can be clearly discerned. No indication of any interaction between the grains of the reactants can be detected. At the position corresponding to the quenched reaction front, the dark Al grains disappear abruptly as a result of melting. The molten Al spreads and covers the Nb grains and the reaction proceeds with the dissolution of solid Nb in the Al liquid matrix and the subsequent precipitation of $NbAl_3$, in the form of small spherical precipitates (diameter <5 μm) disposed all around the unreacted Nb grain cores (Fig. 1c). Moving away from the front, inside the product region, (Fig. 1d), only small amounts of residual Nb and Al can be found between the $NbAl_3$ precipitates, that in turn increased in diameter and agglomerated. The final product is composed only by the phase $NbAl_3$, as confirmed also by the XRPD analysis.

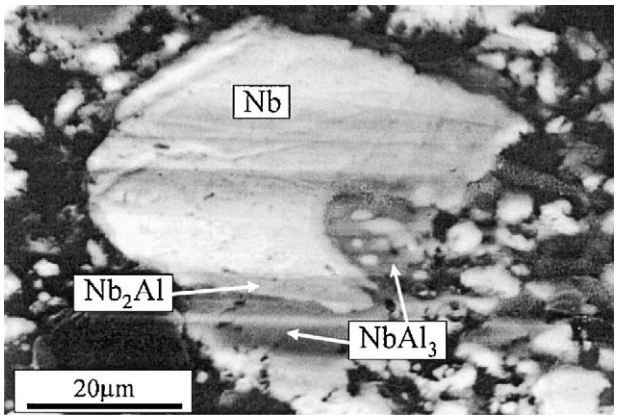

Fig. 2. High magnification of a Nb partially reacted grain obtained from a Nb:Al = 3:1 starting composition (BSE image).

The SEM micrograph in Fig. 2 shows an high magnification image of the morphology of the combustion front zone for a composition much richer in Nb (Nb:Al = 3:1). Also in this case, the molten phase spreads around the Nb grains and the dissolution–precipitation mechanism produces the formation of $NbAl_3$ precipitates around the Nb grain cores. For this composition the consumption of liquid Al to form $NbAl_3$ occurs when a large amount of unreacted solid Nb is still present. The reaction then must proceed through the interaction between the primarily formed $NbAl_3$ and the residual niobium in order to form the Nb-rich phases. In agreement with the above, a layer of a Nb-rich phase (identified as Nb_2Al) between the primarily formed $NbAl_3$ and the residual Nb can be observed in Fig. 2. As confirmed by XRPD results (Table 2) the reaction cannot be completed, and Nb:Al = 3:1 composition, as well as Nb:Al = 2:1

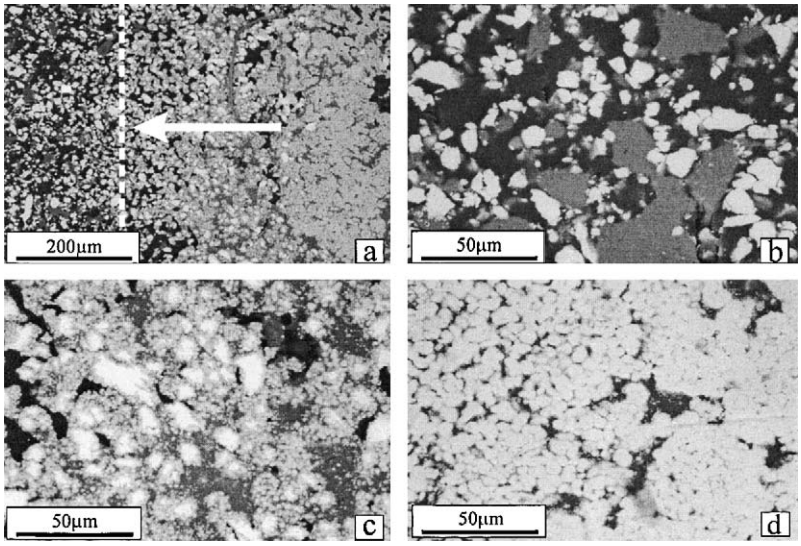

Fig. 1. Microstructure of the quenched product obtained from a Nb:Al = 1:3 starting composition: (a) low magnification image of the quenched front, the arrow indicates the front direction and (b–d) high magnification images of three sample zones. Zone 1: reactants; zone 2: combustion front, zone 3: products. SEM back-scattered image on polished surfaces.

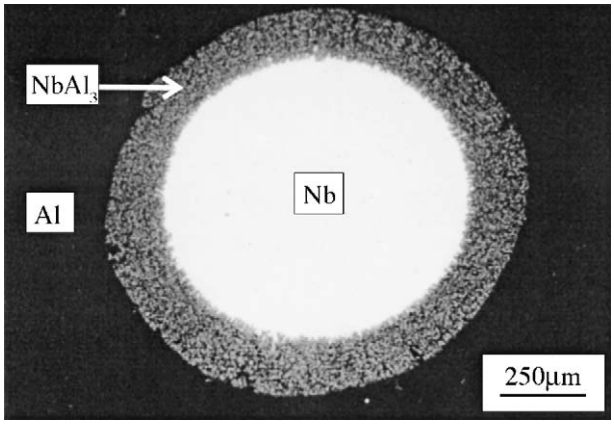

Fig. 3. Microstructure resulting from the reaction between Nb and liquid Al in isothermic conditions: 950 °C, 400 s.

one, give polyphasic products. It is particularly interesting to note as the morphologies observed in the partially reacted samples resemble very closely the microstructure observed when the reaction between solid Nb and liquid Al is conducted in isothermal conditions (Fig. 3).

In the Co–Al system all the reactions developed a stable self-propagating front that proceeded through the entire sample whatever was the Co grain size. The measured combustion front temperature was equal to 1620, 1200, and 1100 °C, respectively, for the compositions Co:Al = 1:1, 2:5, and 2:9. X-ray diffraction analyses performed on the reacted samples indicated that only the combustion of the Co:Al = 1:1 blends produced a single phase (CoAl) product. For the other two compositions investigated (Co:Al = 2:5 and Co:Al = 2:9) the products contain, as the most conspicuous phase, the intermetallic having the same stoichiometry of the green mixture (Table 3) together with small amounts of CoAl and unreacted Al.

Also for the Co–Al system the reaction mechanism was investigated through quenching experiments. Differently from the Nb–Al system, all three compositions are quite rich in aluminum. Al melting occurs as the first step and the reaction is controlled by a dissolution–precipitation mechanism with a phase evolution similar to that described for the Nb:Al = 1:3 reaction.

According to the above results, the possibility of synthesizing a given aluminide by SHS can be discussed on the basis of the corresponding phase diagram and of the reaction temperature. Among the various compositions investigated, only Nb:Al = 1:3 and Co:Al = 1:1 resulted in a single phase product; all the other compositions invariably produced a mixture of aluminides (for the Co–Al system) or a mixture of aluminides plus variable amounts of unreacted elements (for the Nb–Al system). Two causes can be invoked to explain lack of completion of some compositions. The first one is the incongruent melting of some compounds, such as Co_2Al_5 and Co_2Al_9, that must therefore be formed through peritectic reactions, generally considered too slow to be completed in the short times involved in SHS processes. More important is the role played by the liquid phase in the reaction mechanism. Since combustion processes require very high chemical reaction kinetics in order to obtain a steady state propagation, only mechanisms involving liquid phases are generally involved. As a result the kinetic and thermodynamics of the interaction of the solid grain of the transition metal with liquid Al play the main role in controlling the reaction mechanism. The relatively low solubility of the transition metal into the liquid Al (and Si) has already been proven to be responsible for the difficulty of synthesizing various aluminides and silicides with stoichiometries rich in the high melting component [27,33–36]. When reacting aluminum-rich compositions, the dissolution of the transition metal can generally be completed before the saturation of the liquid being obtained and the synthesis of the desired phase can be obtained in one single step characterized by intrinsically fast kinetics. On the contrary, transition metal-rich compositions rapidly saturate the liquid phase causing the precipitation of some Al-rich phase and the consumption of all the liquid phase when large amounts of solid metal grains are still present. Any further advancement of the combustion process requires, per force, the reaction between the primarily precipitated phase and the unreacted metal; this reactions generally involves solid state diffusion (for example solid state diffusion through the Nb_2Al layer in Fig. 2) to be completed. Solid state processes are generally slower than solid–liquid ones and moreover they must be completed in the zone behind the reaction front, where temperature is rapidly decreasing. As a result, Al-poor compositions can be reacted only with great difficulty. SHS processes of this type were shown to be completed only when some form of activation was employed either in the form of an applied electric field [33,34] or through mechanical activation by ball milling of the reactants [35,36]. Both these methods have the scope of reducing the time required for the solid state process to be completed, the first by increasing the reaction temperature and the second by reducing the diffusion distances.

Table 3
Phase composition of the products obtained using starting compositions corresponding to a Co–Al ratio of 2:9, 2:5, and 1:1, respectively

Phases in product	Starting mixture stoichiometry Co:Al		
	2:9	2:5	1:1
Al	t	t	–
Co_2Al_9	M	–	–
Co_2Al_5	–	M	–
CoAl	t	t	M
Co	–	–	–

Relative abundance: M, major; m, minor; t, trace.

3.2. Ignition process

The ignition temperature histories for all the investigated compounds are reported in Figs. 4 and 5 for the Nb–Al system and in Figs. 6 and 7 for the Co–Al system, respectively. All the curves show a plateau at about 645 °C corresponding to the Al melting. A following sharp increase in temperature indicates the ignition of the SHS process.

All the samples reacted in this way were analyzed by X-ray diffraction, scanning electron microscopy, and microprobe analyses, showing that the product formation is in agreement with the SHS experiments previously described (Tables 2 and 3).

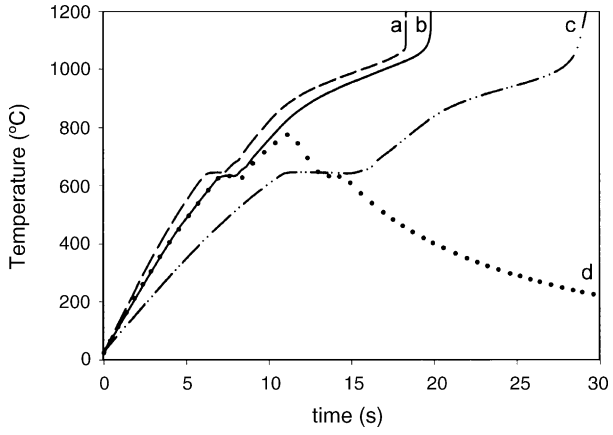

Fig. 4. Temperature profiles characteristic respectively for the compositions Nb:Al = 2:1 (a), Nb:Al = 3:1 (b), Nb:Al = 1:3 (c) and for a quenching test for the composition Nb:Al = 3:1 (d). Nb grain size = −60 mash.

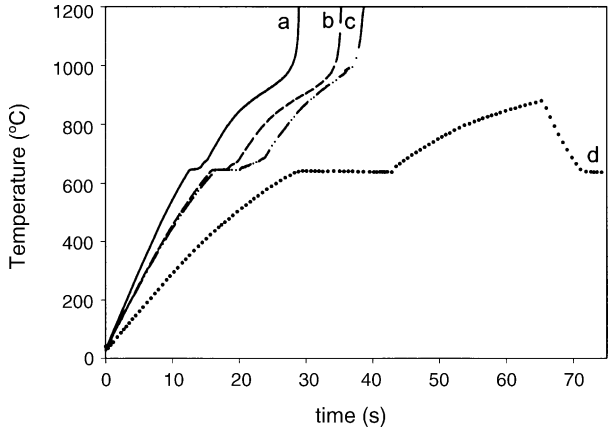

Fig. 5. Temperature profiles characteristic respectively for the compositions Nb:Al = 3:1 (a), Nb:Al = 2:1 (b), Nb:Al = 1:3 (c) and for a quenching test for the composition Nb:Al = 1:3 (d). Nb grain size = −325 mash.

In Fig. 4 the temperature profiles relative to the stoichiometries Nb:Al = 2:1 (a), Nb:Al = 3:1 (b), and Nb:Al = 1:3 (c) for samples prepared with the coarser Nb powders are reported. It must be noted that the combustion process does not start immediately after the melting of Al, but only when the pellet temperature approaches the value of 1100 ± 20 °C (see curves a–c). This result contrast with the common idea that SHS processes in intermetallic systems are triggered by the melting of one of the components. To further confirm this point some experiments have been performed in such a way that the laser heating was stopped when the temperature was just above the melting of Al (Fig. 4, curve d). In this case no ignition was observed. When the finer Nb powder was used, similar results were obtained even if the ignition temperatures resulted to be slightly lower (970 ± 10 °C) (Fig. 5). The laser was set at a power of 40 W for the Nb:Al = 3:1 and Nb:Al = 2:1 compositions, while a power of 50 W was needed to ignite the powder mixture with composition Nb:Al = 1:3.

These results are in good agreement with previous reports [27,29]; these authors also found ignition temperatures for Nb–Al mixtures well above the Al melting point.

Temperature histories for samples of composition Co:Al = 2:5 (a), Co:Al = 1:1 (b), and Co:Al = 2:9 (c) prepared using the coarser Co powders and ignited at a laser power of 40 W are reported in Fig. 6. For all stoichiometries the estimated ignition temperatures are 880 ± 10 °C. Fig. 7 depicts the results obtained testing pellets with the same three compositions but prepared using finer Co particles: for these samples ignition seems to occur just after the Al melting temperature.

In these experiments, the heating transients of the pressed powders is mainly featured by the capability of the irradiated surface to absorb the laser energy and by the pellet heat capacity. For this reason, tests performed on identical compositions and operative conditions can result in different ignition transient when the surface absorptivity is varied by using reactants with different granulometry. This effect is particularly evident for the Co–Al mixtures, as can be observed by comparing Figs. 6 and 7. The heating rate for the pellets containing coarser Co are much lower and the melting plateaus result longer. Numerical simulations of the sample radiant absorptivity (α) and its dependence on temperature were carried out for each test. Coarse Co pellets showed an α value that is much lower (from 40% lower for

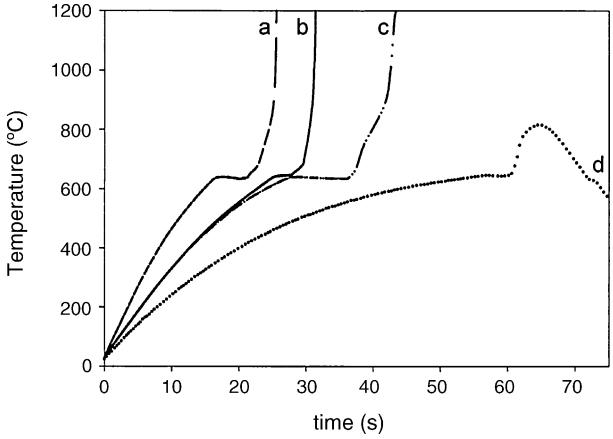

Fig. 6. Temperature profiles characteristic for the compositions Co:Al = 2:5 (a), Co:Al = 1:1 (b), Co:Al = 2:9 (c) and for a quenching test for the composition Co:Al = 1:1 (d). Co grain size = −100 mash.

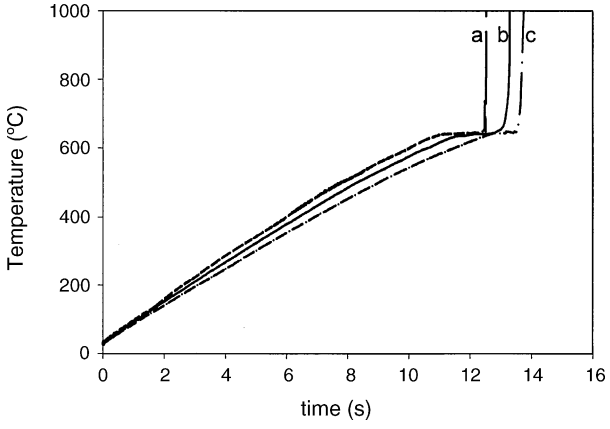

Fig. 7. Temperature profiles characteristic for the compositions Co:Al = 2:5 (a), Co:Al = 1:1 (b), Co:Al = 2:9 (c). Co grain size = <2 μm.

Table 4
Ignition energies

	Starting mixture stoichiometry Co:Al			Starting mixture stoichiometry Nb:Al		
	2:9	2:5	1:1	1:3	2:1	3:1
E_{ig} (kJ/mol$_{at}$)	26 ± 0.5	25 ± 0.5	22 ± 0.5	35 ± 1	29.0 ± 1	27.5 ± 1

Co:Al = 1:1 composition to 50% for the Co:Al = 2:9 one) than for the finer Co ones.

The particular experimental setup used in the present study, that virtually eliminates heat losses by conduction, and the reduced dimension of the samples, allows to simulate the experimental results and to calculate the ignition energies (E_{ig}) by the model reported in [32].

Under the following conditions: (1) the radiant laser energy is the only source driving the heating transient, (2) the temperature distribution in the sample is uniform, (3) the sample heat capacity, emissivity and absorbivity are temperature dependent, (4) melting of the reactants is taking into account, (5) no reaction occurs before ignition, (6) heat loss through the thermocouple can be ignored, the ignition energy can be calculated as:

$$E_{ig} = \int_{t=0}^{t_{ig}} \left[\alpha I_0 - Q_{conv} - Q_{emiss} - \frac{\Delta H_{melt}}{\Delta t_{melt}} \right] dt \quad (1)$$

where t_{ig} is the ignition time, α the sample radiant absorptivity, I_0 the emitted laser power, $Q_{conv}\,dt$ the heat loss by convection, $Q_{emiss}\,dt$ the heat loss by radiation, ΔH_{melt} the latent heat of fusion and Δt_{melt} is the melting time.

On the basis of Eq. (1) the E_{ig} for all the investigated compositions (with the finer metal powders) were calculated and the results are reported in Table 4. For both systems the ignition energy values vary with composition: this effect is due to the different amount of aluminum in the green mixture. Since aluminum melting is accomplished before ignition, compositions richer in aluminum require higher energies.

The significative difference in the ignition behavior observed in the two systems, with the Co–Al mixtures igniting at much lower temperatures even when coarser powders are used, can in principle be explained in different ways. Superficial oxidation of the reactants particles and poor wetting of the solid transition metal by liquid aluminum have been invoked as possible explanation for the unusually high ignition temperature of Nb–Al blends [27,29]. Poor wetting is also considered responsible for the aluminum drop expulsion from the reaction pellets, as described above.

Apart from wettability there is at least another possible explanation for the difference in the ignition behavior that has been largely overlooked. The two systems, in fact, show a very large difference in the solubility of the high melting transition metal into liquid aluminum for temperatures very close to aluminum melting point [14,17]. At 700 °C, for example, the molar solubility of Co in Al is around 1 mol% while that of Nb far less then 0.01%. As a consequence of this large difference in solubility, the dissolution rate of Co is expected to be at least one order of magnitude faster than Nb in the temperature range 700–1000 °C [37,38]. It is therefore no surprising that a temperature significatively higher than aluminum melting point has to be reached, in the case of niobium, to generate enough heat of solution to ignite the SHS process. In this respect the lowering of E_{ig} observed when finer Nb particle size is employed would be a consequence of the increased surface contact area between the reactants that ultimately produces an increase in dissolution rate [39].

4. Conclusions

In the present work, the self-propagating high-temperature synthesis of niobium and cobalt aluminides was investigated. Starting mixtures of stoichiometry corresponding to the following intermetallic compounds were considered: CoAl, Co_2Al_5, Co_2Al_9, Nb_3Al, Nb_2Al, and $NbAl_3$. Only CoAl and $NbAl_3$ could be prepared in pure form while all the other compositions produced polyphasic products. This behavior was addressed to the incongruent nature of some compounds in the Co–Al system and to the different reaction mechanism characterizing the reactivity of rich and poor aluminum mixtures in the Nb–Al system. While Al-rich mixtures propagate through a dissolution–precipitation mechanism, Nb-rich ones propagate through solid state steps leading to incomplete conversion of reactants into products due to the slow kinetic of the solid state diffusion involved.

Ignition of the above SHS reactions was studied in the thermal explosion mode, using CO_2 laser as an external heat source. By employing a suitable model, ignition energy for all compositions could be calculated. Nb–Al mixtures required higher ignition energies than Co–Al ones, also showing ignition temperatures well above the Al melting point. This effect was addressed to the different solubility limits of cobalt and niobium in aluminum.

References

[1] H.A. Lipsitt, in: C.C. Koch, C.T. Liu, N.S. Stoloff (Eds.), High Temperature Intermetallic Alloys, Series, Pittsburg, MRS, 1985.
[2] D.J. Duquette, Mater. Sci. Eng. A198 (1995) 205.
[3] V. Gauthier, F. Bernard, E. Gaffet, C. Josse, J.P. Larpin, Mater. Sci. Eng. A272 (1999) 334.
[4] D.L. Anton, D.M. Shah, Mater. Sci. Eng. A153 (1992) 402.
[5] D.L. Anton, D.M. Shah, Mater. Res. Soc. Symp. 213 (1991) 733.
[6] S. Dymek, M. Dollar, K. Leonard, Mater. Sci. Eng. A239–A240 (1997) 507.
[7] A. Dollar, S. Dymek, Intermetallics 11 (2003) 341.
[8] H.A. Lipsitt, in: S.M. Aller, R.M. Pelloux, R. Widmer (Eds.), Advanced High Temperature Alloys: Processing and Properties, ASM International, Materials Park, OH, 1986, p. 231.
[9] N.R. Shivaparan, M.A. Teter, R.J. Smith, Surf. Sci. 476 (2001) 152.
[10] P. LeClair, H.J.M. Swagten, J.T. Kohlhepp, W.J.M. de Jonge, Appl. Phys. Lett. 76 (2000) 3782.
[11] J.F. Bobo, F.B. Mancoff, K. Bessho, M. Sharma, K. Sin, D. Guarisco, S.X. Wang, B.M. Clemes, J. Appl. Phys. 83 (1998) 6685.
[12] F.Z. Cui, J.F. Wang, Y.D. Fan, H.D. Li, J. Appl. Phys. 70 (1991) 3379.

[13] M. Tanaka, N. Ikarashi, H. Sakakibara, K. Ishida, T. Nishinaga, Appl. Phys. Lett. 60 (1992) 835.
[14] T.B. Massalski (Ed.), Binary Alloy Phase Diagrams, vol. 2, American Society for Metals, Materials Park, OH 44073, 1986.
[15] R.L. Fleischer, R.D. Field, K.K. Denike, R.J. Zabala, Metall. Trans. 21A (1990) 3063.
[16] D.K. Tappin, L.S. Smith, D.N. Horspool, M. Aindow, Acta Mater. 45 (1997) 4923.
[17] M. Hansen, K. Anderko, Constitution of Binary Alloys, Metallurgy and Metallurgical Engineering Series, McGraw-Hill Book Company, 1958.
[18] S. Miura, C.T. Liu, Intermetallics 2 (1994) 297.
[19] S. Dymek, S.J. Hwang, M. Dollar, J.S. Kallend, P. Nash, Scripta Metall. 27 (1992) 661.
[20] Z. Peng, C. Suryanarayana, F.H. Froes, Metall. Mater. Trans. 27A (1996) 41.
[21] R.D. Field, D.F. Lahrman, R. Darolia, Acta Metall. 39 (1991) 2951.
[22] C.R. Kachelmier, J.P. Lebrat, A. Varma, P.J. McGinn, in: B. Farouk, M.P. Pinar Menguc, R. Viskanta, C. Presser, S. Chellaiah (Eds.), Heat Transfer in Fire and Combustion Systems, ASME, New York, 1993, pp. 271–276.
[23] Y.S. Naiborodenko, V.I. Itin, A.G. Merzhanov, I.P. Borovinskaya, V.P. Ushakov, V.M. Maslov, Sov. Phys. J. 16 (1973) 872.
[24] V.V. Boldyrev, V.V. Aleksandrov, M.A. Khorchagin, B.P. Tolochko, S.N. Gusenko, A.S. Solov, Dokl. Akad. Nauk. SSSR 259 (1981) 1127.
[25] H.Y. Yi, A. Petric, J.J. Moore, J. Mater. Sci. 27 (1992) 6797.
[26] W.C. Lee, K.C. Hsu, S.L. Chung, J. Self-Propagating High-Temp. Synth. 4 (1995) 95.
[27] C.R. Kachelmier, A.S. Rogachev, A. Varma, J. Mater. Res. 10 (1995) 2260–2270.
[28] A. Varma, C.R. Kachelmyer, A.S. Rogachev, Int. J. Self-Propagating High-Temp. Synth. 5 (1996) 1.
[29] V.M. Maslov, I.P. Borovinskaya, M.Kh. Ziatdinov, Combust. Explos. Shock Waves 15 (1979) 41.
[30] Y.S. Naiborodenko, G.V. Lavrenchuk, V.M. Filatov, Sov. Powder Metall. Met. Ceram. (Engl. Trans.) 21 (1987) 909.
[31] U. Anselmi-Tamburini, M. Arimondi, F. Maglia, G. Spinolo, Z.A. Munir, J. Am. Ceram. Soc. 81 (1998) 1765.
[32] M. Monagheddu, N. Bertolino, P. Giuliani, C. Zanotti, U. Anselmi-Tamburini, J. Appl. Phys. 92 (2002) 594.
[33] S. Gedevanishvili, Z.A. Munir, Mater. Sci. Eng. A211 (1996) 1.
[34] F. Maglia, U. Anselmi-Tamburini, N. Bertolino, C. Milanese, Z.A. Munir, J. Mater. Res. 16 (2001) 534.
[35] F. Maglia, C. Milanese, U. Anselmi-Tamburini, S. Doppiu, G. Cocco, J. Mater. Res. 17 (2002) 1992.
[36] F. Maglia, C. Milanese, U. Anselmi-Tamburini, S. Doppiu, G. Cocco, Z.A. Munir, J. Alloys Compd. 385 (2004) 269.
[37] C. Milanese, Ph.D. Thesis, University of Pavia, 2001.
[38] V.N. Yeremenko, Y.N. Natanzov, V.Y. Dybkov, J. Less-Common Met. 50 (1976) 29.
[39] U. Anselmi-Tamburini, F. Maglia, S. Doppiu, M. Monagheddu, G. Cocco, Z.A. Munir, J. Mater. Res. 19 (2004) 1558.